

SCIENTIFIC REPORTS

OPEN

Transcriptomic analysis of the liver of cholesterol-fed rabbits reveals altered hepatic lipid metabolism and inflammatory response

Weirong Wang^{1,2}, Yulong Chen³, Liang Bai^{1,2}, Sihai Zhao^{1,2}, Rong Wang^{1,2}, Baoning Liu^{1,2}, Yali Zhang^{1,2}, Jianglin Fan⁴ & Enqi Liu^{1,2}

Rabbits are a suitable animal model for atherosclerosis due to their sensitivity to dietary cholesterol. Moreover, rabbits have lipoprotein profiles that are more similar to humans than those of other laboratory animals. However, little is known about the transcriptomic information related to atherosclerosis in rabbits. We aimed to determine the changes in the livers of rabbits fed a normal chow diet (control) or high cholesterol diet (HCD) by histological examinations and RNA sequencing analysis. Compared with the control group, the lipid levels and small LDL subfractions in plasma were increased, and aortic atherosclerotic plaques were formed in the HCD group. Most importantly, HCD resulted in lipid accumulation and inflammation in the livers. Transcriptomic analysis of the liver showed that HCD induces 1183 differentially expressed genes (DEGs) that mainly participate in the regulation of inflammation and lipid metabolism. Furthermore, the signaling pathways involved in inflammation and lipid metabolism were enriched by KEGG pathway analysis. In addition, hepatic DEGs of the HCD group were further validated by real-time PCR. These results suggest that HCD causes liver lipid accumulation and inflammatory response. Although the relationships between these hepatic changes and atherogenesis need further investigation, these findings provide a fundamental framework for future research on human atherosclerosis using rabbit models.

Atherosclerosis is a complex multifactorial disease of the aorta and muscular arteries and the leading cause of morbidity and mortality throughout the world¹. Many laboratory animal models have been used to study the process of atherogenesis, including mice, rabbits, pigs and nonhuman primates. In particular, mouse models are widely used due to the relatively short time frame for the progression of atherosclerosis and the relative ease of genetic manipulation². While not all aspects of mouse atherosclerosis are identical to humans, several characteristics of lipid metabolism in rabbits make them particularly suitable for the study of human hypercholesterolemia and atherosclerosis. First, a large body of evidence suggests that high levels of plasma cholesterol, especially low-density lipoprotein (LDL)-cholesterol, result in atherosclerotic lesion formation in humans³. Unlike mice, in which high-density lipoproteins (HDLs) are the predominant plasma lipoproteins, rabbit lipoprotein profiles are LDL-rich, similar to those of humans^{4,5}. Second, it has been reported that cholesteryl ester transfer protein (CETP) plays a central role in lipid metabolism and atherosclerotic processes⁶. Rabbits have abundant CETP activity in the plasma as do humans, whereas mice do not have an endogenous CETP gene^{7,8}. Third, rabbits do not have hepatic ApoB mRNA editing activity as humans, so rabbit ApoB-48 is only present in chylomicrons as in humans. However, ApoB-48 is present in all ApoB-containing particles such as very low-density lipoproteins (VLDLs), LDLs and chylomicrons in mice⁹. In addition, hepatic lipase (HL), which plays a major role in lipoprotein metabolism, is bound to the vascular endothelium in rabbits and humans, whereas the majority of HL is circulating in the plasma in mice^{10,11}. Therefore, rabbits provide a unique system to study the initiation

¹Research Institute of Atherosclerotic Disease, Xi'an Jiaotong University Cardiovascular Research Center, Xi'an, Shaanxi, 710061, China. ²Laboratory Animal Center, Xi'an Jiaotong University Health Science Center, Xi'an, Shaanxi, 710061, China. ³Shaanxi Key Laboratory of Ischemic Cardiovascular Disease, Institute of Basic and Translational Medicine, Xi'an Medical University, Xi'an, Shaanxi, 710021, China. ⁴Department of Molecular Pathology, Interdisciplinary Graduate School of Medicine and Engineering, University of Yamanashi, Yamanashi, 409-3898, Japan. Correspondence and requests for materials should be addressed to E.L. (email: liuenqi@mail.xjtu.edu.cn)

Received: 20 October 2017

Accepted: 10 April 2018

Published online: 24 April 2018

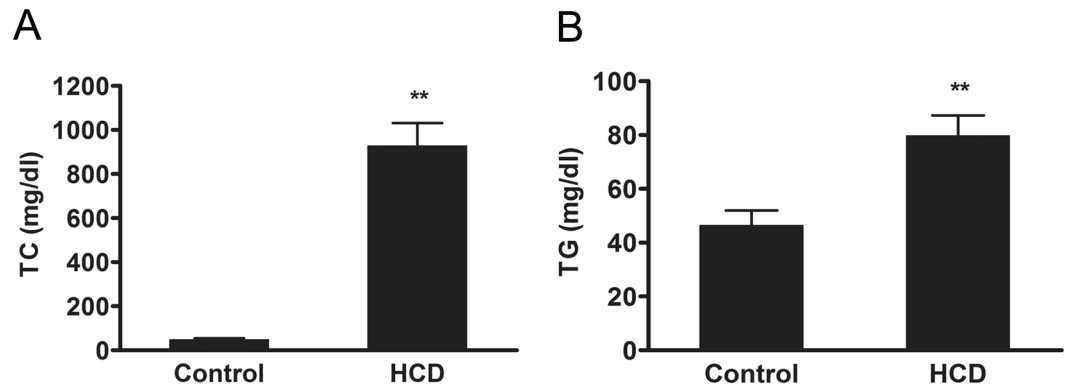


Figure 1. The plasma lipid levels in rabbits. The rabbits were fed a normal chow diet or 0.3% high cholesterol diet for 16 weeks. The plasma levels of TC and TG were measured. Data are expressed as the mean \pm SEM. $n = 10$ for each group. ** $P < 0.01$ vs. the control group.

and progression of atherosclerosis in humans. Despite the importance of rabbit models for the study of human hypercholesterolemia and atherosclerosis, little is known about the transcriptomic information related to atherosclerosis in rabbits.

Next-generation sequencing platforms have made genomic and transcriptomic analyses affordable for researchers to elucidate the molecular mechanisms of human diseases. RNA sequencing (RNA-Seq) uses massively parallel sequencing to analyze the transcriptome at higher resolution than Sanger sequencing- and microarray-based methods^{12,13}. We envision that investigation of the transcriptomics in rabbits fed a high cholesterol diet can provide a better understanding of the biochemical and molecular processes involved in the initiation and progression of atherosclerosis in this model.

Therefore, in the present study, we conducted RNA-Seq analysis of livers in rabbits fed a high cholesterol diet coupled with analyses of the plasma lipids and lipoprotein subfractions, aortic atherosclerotic lesions and liver pathology.

Results and Discussion

Plasma lipid levels and lipoprotein subfractions. Compared with the normal chow diet (control) group, the plasma levels of total cholesterol (TC) and triglycerides (TG) were increased by 19.4-fold and 1.7-fold in high cholesterol diet (HCD)-fed rabbits for 16 weeks, respectively (Fig. 1, $P < 0.01$).

As shown in Fig. 2, plasma lipoprotein subfraction analysis showed that the levels of VLDLs, intermediate-density lipoproteins (IDLs) and LDLs were markedly increased in the HCD group compared with the control group. It is well established that increased LDL levels are considered a major risk factor for atherosclerosis^{14,15}. However, an increasing number of studies have found that the disproportionate number of small and denser LDL particles is an independent risk factor for cardiovascular diseases because small LDL particles may reside longer in circulation and may be more prone to uptake by macrophages in atherosclerosis^{16,17}. Therefore, we further analyzed the size distribution of LDL particles using the Lipoprint LDL System. The system can resolve plasma lipoproteins to discrete bands consisting of VLDL; IDL bands A, B, and C; LDL subfractions 1 to 7. Subfraction 1 represents large LDL particles, subfraction 2 indicates intermediate LDL particles, and subfractions 3–7 refer to small LDL particles¹⁸. We found that small LDL particles were basically not present in the control rabbits whereas they (fractions 3–4) were dramatically increased in the HCD-fed rabbits (Fig. 2C). It has been reported that small LDL particles are more atherogenic than large buoyant LDL particles^{19,20}. Recent clinical trials also showed that small LDL particles were markers of early atherosclerosis, and the measurement of small LDL particles provided important information in the risk assessment for atherosclerotic disease^{21,22}. In addition, there were obvious differences in the plasma levels of VLDL, IDL-C, IDL-B and IDL-A between the HCD group and the control group in our study ($P < 0.01$). Data from the present study showed that high dietary cholesterol increased the plasma levels of TC and TG, and increased plasma TC levels were mainly caused by elevated small LDL particles in rabbits.

Gross and histological changes in atherosclerotic lesions. Gross atherosclerotic lesions and histological features in the aorta were examined. Aortas of rabbits were collected and stained with Sudan IV. Compared with the control group, which contained no visible lesions, *en face* lesions in the HCD group were remarkable and distributed from the aortic arch, thoracic aorta to abdominal aorta with predominance in the aortic arch (Fig. 3A).

To further analyze the histological changes of atherosclerotic lesions, we examined the intimal lesions in the aortic arch using hematoxylin and eosin (H&E) and Elastica van Gieson (EVG) staining. We found that the intimal lesions were mainly composed of macrophage-derived foam cells, whereas no lesions were found in the control group (Fig. 3B). It is generally accepted that the enhancement of intimal macrophage (M Φ) accumulation may increase the vulnerability of the plaques or make the plaques prone to rupture, leading to thrombosis in atherosclerosis²³. In addition, vascular smooth muscle cell (SMC) proliferation also plays a crucial role in the progression of atherosclerosis²⁴. Immunohistochemical staining showed that in addition to macrophages, the

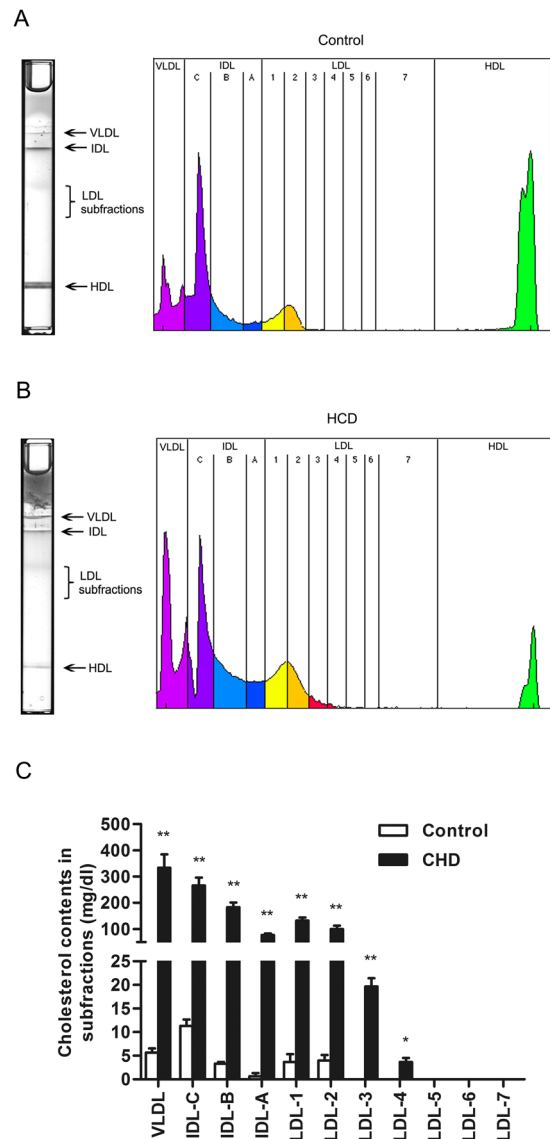


Figure 2. The plasma lipoprotein subfraction analysis in rabbits. Blood samples in the control group and HCD group were used for lipoprotein subfraction analysis. Data are expressed as the mean \pm SEM. $n = 3$ for each group. * $P < 0.05$ and ** $P < 0.01$ vs. the control group.

lesions also contained many SMCs (Fig. 3C). Thus, aortic atherosclerotic lesions were well formed in rabbits fed a 0.3% cholesterol diet for 16 weeks.

Histological changes in liver. Accumulating evidence suggests that the liver plays a key role in the inflammatory response evoked by dietary cholesterol. Clinical studies found that liver-derived inflammation markers such as C-reactive protein and serum amyloid A (SAA) were rapidly increased after consumption of an excess amount of dietary cholesterol, thereby promoting the onset of early aortic lesion formation^{25,26}. These results indicated that liver plays a key role in the inflammatory response evoked by dietary constituents. We found that there were significant steatosis, ballooning and inflammation in the HCD group compared with the control group (Fig. 4A). In addition, histological scoring for inflammation was based on the Brunt classification^{27,28}. There was a trend toward higher inflammation in the HCD group compared with the control group ($P < 0.01$) (Fig. 4B). The results of Oil Red O revealed clear lipid accumulation and severe macrovesicular hepatic steatosis in the HCD group compared with the control group (Fig. 4C and D). These results suggest that HCD could cause fatty degeneration and inflammatory response in the liver. In support of our observations, it has been shown that dietary cholesterol induced pro-inflammatory gene expression in the livers of ApoE*3Leiden transgenic mice²⁹.

RNA-Seq analysis of hepatic gene expression. To gain insight into the complex traits underlying the pathophysiological response of the liver to dietary cholesterol, transcriptomic analysis was performed by RNA-Seq. In the previous study, we identified the gene mutations or modifiers through whole-genomic sequencing and deep transcriptome sequencing of LDL receptor deficient (WHHL) rabbits and cholesterol-fed New

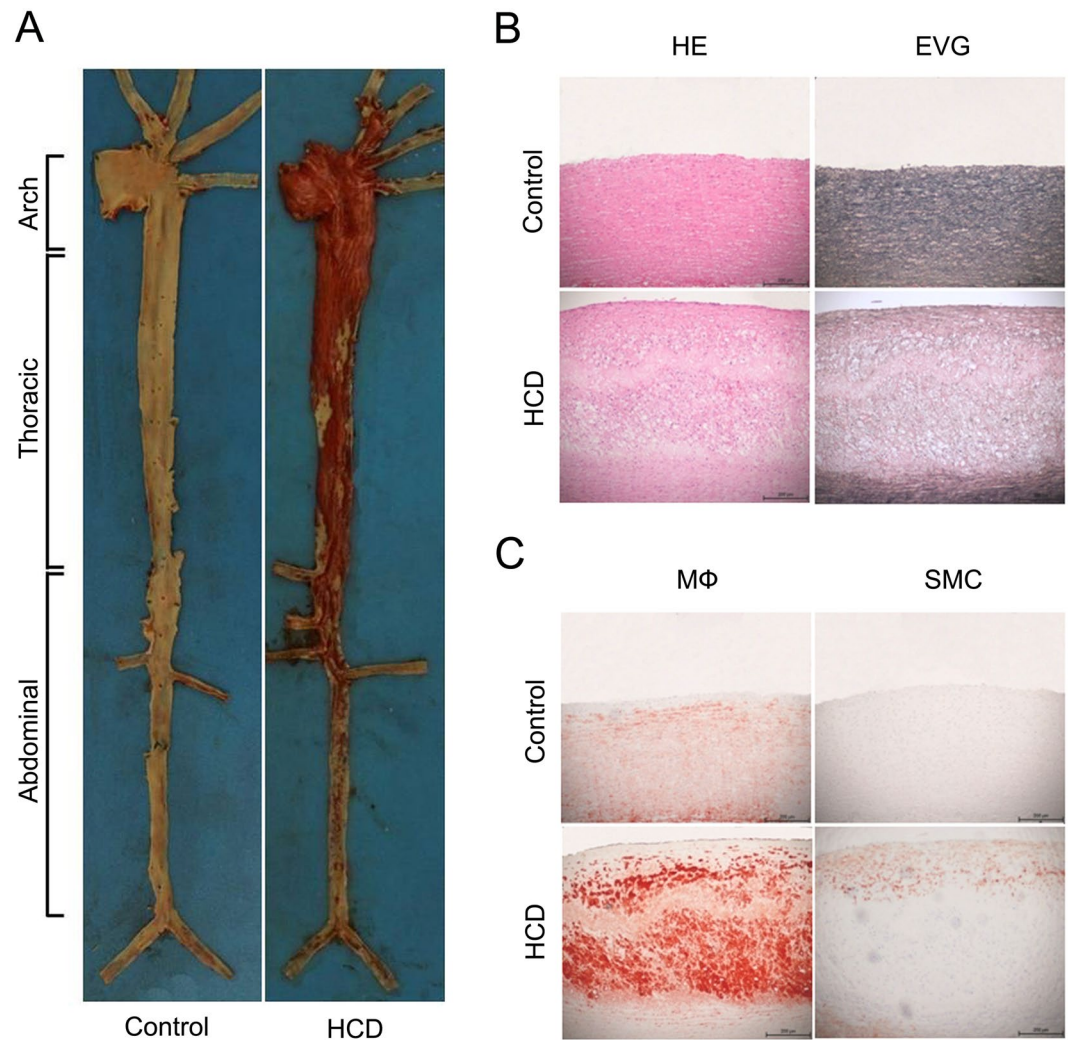


Figure 3. Gross and histological changes in atherosclerotic lesions in rabbits. **(A)** Representative pictures of Sudan IV staining in aortas. **(B)** The aortic atherosclerotic lesions were stained with H&E or EVG. **(C)** The aortic atherosclerotic lesions were stained with antibodies against MΦ or SMC by immunohistochemistry. Bar = 200 μ m.

Zealand White rabbits. The previous study mainly addressed transcriptional changes in the WHHL rabbits, while cholesterol-fed New Zealand White rabbits were used as a reference³⁰. To further emphasize the relationship with lipoprotein profiles and aortic atherosclerosis, in the current study, we focused on the hepatic gene expression changes and liver pathology in the setting of hepatic steatosis induced by cholesterol diet in the Japanese White rabbits. The transcriptomic analysis revealed that there were 1,183 differentially expressed genes (DEGs) compared with the control rabbits. Of them, 984 genes were up-regulated and 199 genes were down-regulated compared with the control group (Supplementary Table S1). Kleemann *et al.* found that 1,896 genes were significantly changed in the livers of ApoE*3Leiden mice fed a cholesterol diet during atherogenesis by GeneChip microarrays²⁹. To investigate the functions of these 1,183 DEGs, we grouped them into five categories according to their functions, including glucose metabolism, lipid metabolism, protein metabolism, cell proliferation/apoptosis and inflammation. Our results revealed that HCD predominantly affected genes involved in inflammation and lipid metabolism in the liver (Fig. 5 and Supplementary Table S2). As shown in Fig. 5 and Table S1, we found that the adaptation of hepatic lipid metabolism to dietary cholesterol was mainly controlled by the genes of cholesterol biosynthesis and lipid metabolism. Sterol regulatory element binding protein 1 (SREBF1), a key transcriptional factor in modulating cholesterol biosynthesis, was up-regulated 40.7-fold compared to the control rabbits. Karasawa *et al.* revealed that hepatic SREBP1 determined plasma remnant lipoproteins and contributed to atherosclerosis in LDLR^{-/-} mice³¹. It has been reported that 24-dehydrocholesterol reductase (DHCR24) is likely a target for SREBPs, which has been suggested to regulate the genes involved in cholesterol biosynthesis³². Our results showed that the DHCR24 gene was down-regulated 2.1-fold in HCD-fed rabbits. Furthermore, HCD induced many genes that mediate the inflammatory response in the liver. These genes include proteases (MMP2, MMP14, MMP15, TIMP1, TIMP2, TIMP3), chemokines (CCL25, CCL21, CXCL16, MIF), adhesion molecules (CD74, CD14, CD97, ICAM1) and cardiovascular risk factors (SAA3, CEBPB). It is generally accepted

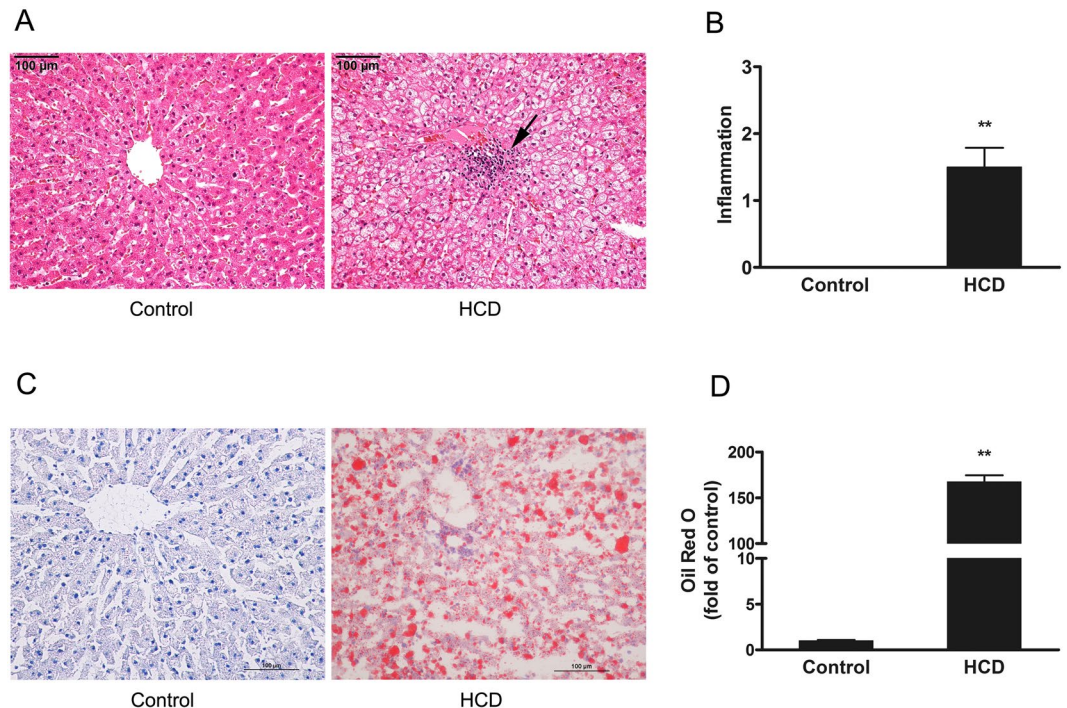


Figure 4. Histological changes in the livers of rabbits by H&E and Oil Red O staining. (A) Compared to the control liver, the hepatocytes of HCD-fed rabbits show fatty degeneration and accumulation of mononuclear infiltration in the center (indicated by an arrow). (B) Hepatic inflammation was quantified using the Brunt classification. (C) Representative Oil Red O staining of livers in the control group and HCD group. (D) Oil Red O staining area was measured using the WinROOF image analysis software. Data are expressed as the mean \pm SEM. $n = 4$ for each group. $**P < 0.01$ vs. the control group. Bar = 100 μm .

that atherosclerosis is a multifactorial and persistent condition and is regarded as a form of chronic inflammation induced by lipid accumulation³. Other studies showed that there is a link between cholesterol and inflammation in ApoE^{-/-} mice and ApoE^{*3}Leiden mice fed with high cholesterol^{29,33}. Taken together, these findings suggest that hepatic lipid metabolism and inflammation may be closely associated with the initiation and progression of atherosclerosis in rabbits.

The Kyoto Encyclopedia of Genes and Genomes (KEGG) pathway analysis provided additional possible functional information showing the pathways relevant to DEGs during atherogenesis. In concordance with our DEG results, analysis of the KEGG pathway showed that these DEGs were mainly contained in lipid metabolism- and inflammation-related signaling pathways including PI3K-Akt, MAPK, ABC transporters, FoxO, PPAR, AMPK, NF- κ B, mTOR, tumor necrosis factor (TNF), Toll-like receptor and cGMP-PKG signaling pathways. Significantly, HCD activated specific inflammatory pathways, such as NF- κ B, Toll-like receptor and TNF signaling pathways in rabbits (Fig. 6 and Supplementary Table S3). As shown in Fig. 6, the number and percentage of DEGs in these signaling pathways were analyzed. We found that the largest functional pathway was the MAPK signaling pathway, representing a total of 21 DEGs (~12% of the total). It has been reported that these enriched signaling pathways participate in the inflammatory response and lipid metabolism in atherosclerosis^{34,35}. Vergnes *et al.* also discovered that the hepatic inflammatory response was evoked by high cholesterol feeding in LDLR^{-/-} mice³⁶. These above studies suggest that the uptake of dietary cholesterol leads to the inflammatory response of the liver in rabbits.

Quantitative real-time PCR analysis. Both hypercholesterolemia and inflammatory response are well-known risk factors for the development of atherosclerosis and have been shown to play a causal role in the progression of atherosclerotic plaques³. To validate the DEGs in the liver, real-time PCR was carried out. As shown in Fig. 7, the genes SREBF1, LDLR and CYP7A1 involved in lipid metabolism were significantly changed in the livers of the HCD group compared with the control group. Furthermore, we found that the expression levels of inflammatory genes MMP2, TIMP1, MIF, ICAM1 and SAA3 were increased, whereas the expression level of interleukin-1R2 (IL-1R2) was decreased. Previous studies showed that the proinflammatory cytokine IL-1 interacts with cells through two types of receptors, type I receptor (IL-1R1) and IL-1R2. IL-1R2 inhibits IL-1 activity by acting as a decoy target for IL-1^{37,38}. These results indicate that dietary cholesterol can be an important trigger and a possible source of the inflammatory component.

The correlation was calculated to compare the expression levels between RNA-Seq and real-time PCR. Fold changes in DEGs between the two techniques were significantly correlated in the depot (Pearson's $R = 0.88$) (Fig. 8). The results confirmed that these DEGs identified in our study were very reliable.

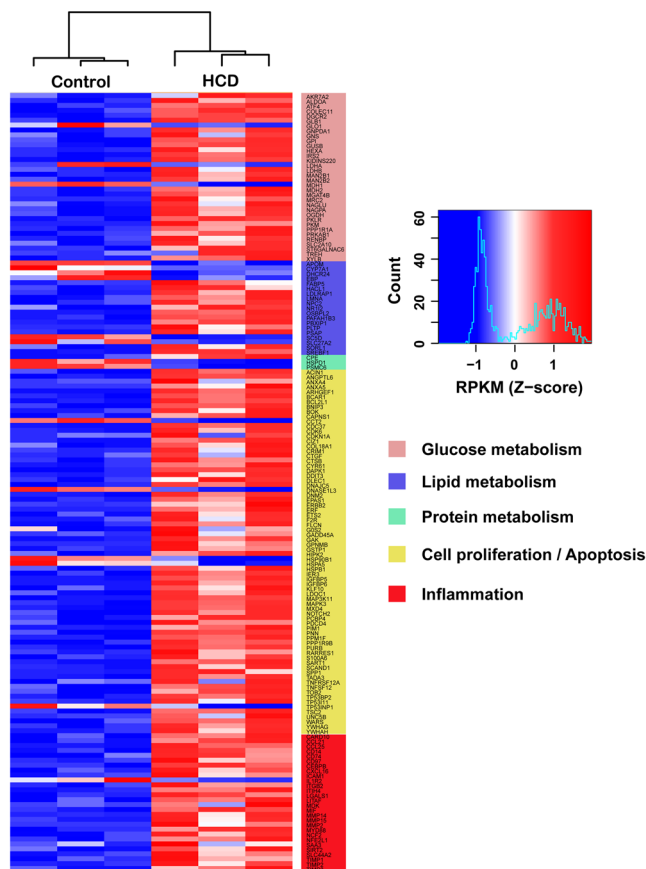


Figure 5. General features of differentially expressed genes in the livers of rabbits. The DEGs were analyzed using DESeq software by comparing the control and HCD groups. Expression intensities are displayed from blue (low expression) to red (high expression), and the expression level is proportional to the brightness of the color (see color bar). n = 3 for each group.

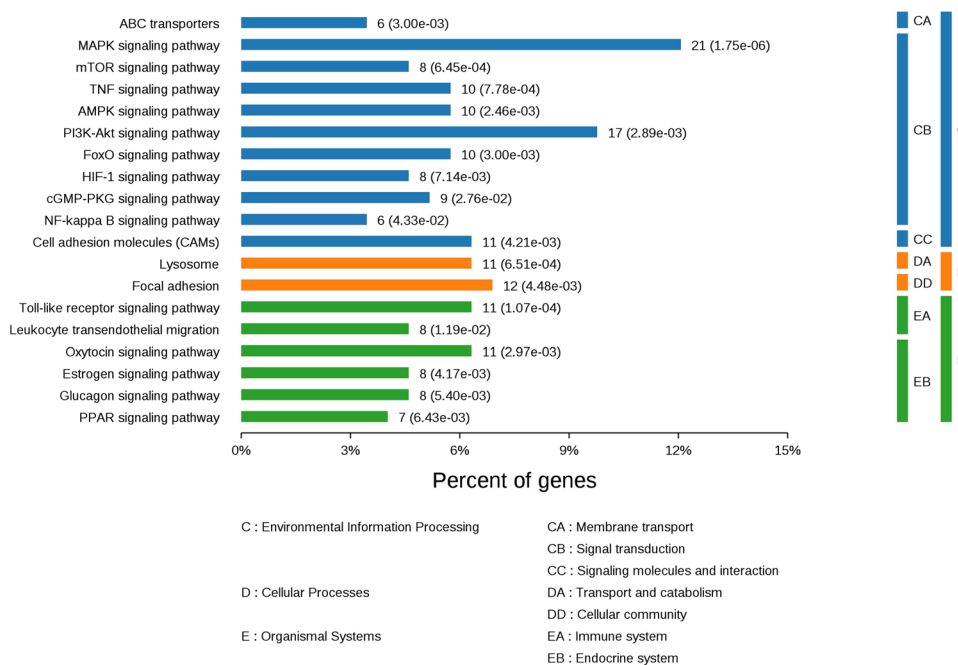


Figure 6. Enriched KEGG pathways of differentially expressed genes in the livers of rabbits. The DEGs were mapped into the KEGG databases, significantly enriched KEGG terms were determined by $P \leq 0.05$. n = 3 for each group.

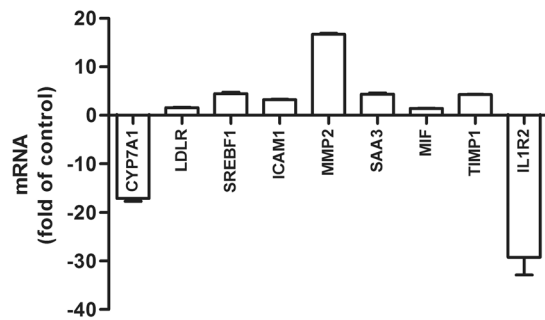


Figure 7. Quantitative real-time PCR verification. Real-time PCR was performed essentially to validate the DEGs in the livers of the control group and HCD group. Data are expressed as the mean \pm SEM. $n = 3$ for each group.

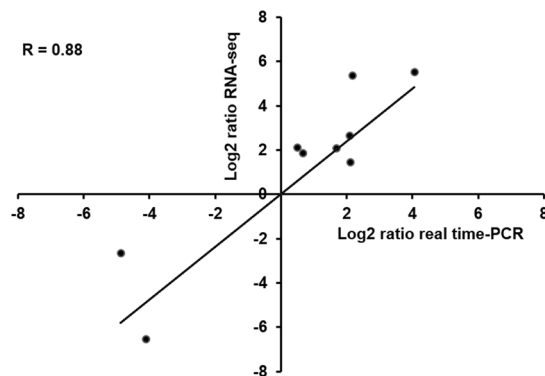


Figure 8. The correlation of log₂-fold change in gene expression in the liver of rabbits between the RNA-Seq and real time-PCR.

Conclusions

The results from the current study demonstrate that dietary cholesterol is not only a risk factor for hypercholesterolemia but also a trigger of hepatic inflammation. Although the significance of hepatic inflammation in the development of atherosclerosis deserves further investigation, these results provide valuable information for the study of both hypercholesterolemia and hepatic inflammation using rabbit models. Further studies are ongoing to validate these findings.

Materials and Methods

Animals and diets. Male Japanese White rabbits (2.5–3.0 kg) were provided by the Laboratory Animal Center of Xi'an Jiaotong University. In the current study, we aimed to determine the influence of hypercholesterolemia on transcriptomic change and liver pathology that may be related to atherosclerosis in rabbits. It is well known that rabbits are sensitive to dietary cholesterol and rapidly develop severe hypercholesterolemia leading to atherosclerosis⁵. However, rabbits are out-bred and show a wide biological variability in terms of individual responsiveness to dietary cholesterol³⁹. To minimize the intra-group variations of transcriptomic analysis caused by different response to a cholesterol diet, thirty rabbits were fed a chow diet containing 0.5% cholesterol for one week. To ensure that all rabbits had a similar responsiveness to cholesterol feeding, we selected rabbits based on the plasma levels of TC (ranging from 300 to 500 mg/dl). Eventually, twenty rabbits were selected and subsequently divided into two groups: normal chow diet group and cholesterol diet group fed a 0.3% cholesterol diet. All rabbits were given a restricted diet of 100 g/day for 16 weeks. Rabbits were individually housed in metal cages in air-conditioned rooms under a 12 h light/12 h dark cycle and were given free access to water throughout the experiments. The experimental protocol was in accordance with the National Institutes of Health Guide for Care and Use of Laboratory Animals and was approved by the Laboratory Animal Care Committee of Xi'an Jiaotong University.

Biochemical analysis. Blood samples were collected from the ear artery of rabbits after fasting for 16 h. The plasma levels of TC and TG were measured using commercial kits (Biosino Bio-technology and Science, Beijing, China). Plasma samples were also used for lipoprotein subfraction analysis. The analysis was performed electrophoretically using high-resolution 3% polyacrylamide gel tubes and the Lipoprint LDL System (Quantimetrix Corporation, Redondo Beach, CA, USA) according to the manufacturer's instructions as previously described^{40,41}.

Determination of atherosclerotic lesions. Rabbits were sacrificed with an injection of phenobarbital sodium and xylazine hydrochloride. The aortic tree was isolated, opened longitudinally, fixed in 10% neutral buffered formalin, and stained with Sudan IV⁴². Then, the aortic arch was cut into 10 sections. The sections were embedded in paraffin and cut into 5- μ m thick serial sections, stained with H&E and EVG. For the evaluation of cellular components in atherosclerotic lesions, the sections were immunohistochemically stained with antibodies against RAM11 (macrophage marker) (Dako, Carpinteria, CA, USA) and HHP35 (SMC marker) (Thermo, Rockford, IL, USA).

Histology and Immunohistochemistry. The livers were fixed in 10% neutral buffered formalin and processed for embedding in paraffin. Then, specimens were cut into 5- μ m thick serial sections and stained with H&E. Frozen sections of liver (5- μ m thick) were stained with Oil Red O for evaluation of hepatic fatty change. The Oil Red O staining area was measured using the WinROOF image analysis software (Mitani, Tokyo, Japan).

Total RNA extraction and cDNA library construction. Total RNA was extracted from the liver using RNazol (Takara, Tokyo, Japan). RNA concentrations and purity were determined using Nanodrop (Thermo, Rockford, IL, USA), and integrity was verified using an Agilent 2100 Bioanalyzer (Agilent Technologies, Santa Clara, CA, USA). mRNA was purified from total RNA using the NEBNext[®] Poly(A) mRNA magnetic isolation module. A total of 6 paired-end libraries were constructed using a NEBNext UltraTM RNA Library Prep Kit following Illumina manufacturer's recommendation. Library quality was assessed on the Agilent Bioanalyzer 2100 system. The clustering of the index-coded samples was performed on a cBot Cluster Generation System using TruSeq PE Cluster Kit v4-cBot-HS (Illumina). The libraries were sequenced on an Illumina HiSeq. 2500 platform with 100 bp paired-end reads (Illumina, San Diego, CA, USA).

Differentially expressed gene analysis. The Perl script was used to trim the reads with contaminated adapters, more than 20% low-quality bases (Phred quality score < 20), and more than 10% Ns. First, we obtained clean reads (Supplementary Table S4). Then, clean reads were aligned to the rabbit reference genome (GCA_000003625) using TopHat. The gene expression was quantified and normalized by Cufflinks in RPKM (reads per million per kilo bases)⁴³. The DEGs were analyzed using DESeq software by comparing the control and HCD groups⁴⁴. The significance threshold of the *p*-value in multiple tests was set by the false discovery rate (FDR). The threshold, the absolute values of fold change ≥ 2 and FDR < 0.05, was applied to judge the significance of gene expression. For the functional and pathway enrichment analysis, the DEGs were then mapped into the KEGG databases, and significantly enriched KEGG terms were determined by $P \leq 0.05$.

Real-time PCR. Real-time PCR was performed essentially to validate and confirm the differences in gene expression between the HCD group and the control group. Total RNA was extracted from the liver using RNazol. cDNAs were synthesized using a RevertAid First Strand cDNA Synthesis Kit (Takara, Tokyo, Japan) following the manufacturer's instructions. Real-time PCR was performed with the SYBR Green PCR master mix (Takara, Tokyo, Japan) using a thermal cycler dice real time system. Primers were designed with primer premier 5.0 (Premier Biosoft, Palo Alto, CA, USA) (Supplementary Table S5). GAPDH was used as an endogenous control. The relative gene expression was quantitatively analyzed by the comparative Ct method ($2^{-\Delta\Delta CT}$). Data were normalized to rabbit GAPDH mRNA levels.

Statistical analysis. Data are presented as the mean \pm SEM. Statistical analysis was performed by the two-tailed Student's *t*-test using GraphPad Prism software. Differences between groups were considered statistically significant if $P < 0.05$.

References

- Libby, P., Ridker, P. M. & Hansson, G. K. Progress and challenges in translating the biology of atherosclerosis. *Nature*. **473**, 317–325 (2011).
- Getz, G. S. & Reardon, C. A. Animal models of atherosclerosis. *Arterioscler Thromb Vasc Biol*. **32**, 1104–1115 (2012).
- Glass, C. K. & Witztum, J. L. Atherosclerosis: the road ahead. *Cell*. **104**, 503–516 (2001).
- Ylä-Herttuala, S. *et al.* Evidence for the presence of oxidatively modified low density lipoprotein in atherosclerotic lesions of rabbit and man. *J Clin Invest*. **84**, 1086–1095 (1989).
- Fan, J. *et al.* Rabbit models for the study of human atherosclerosis: From pathophysiological mechanisms to translational medicine. *Pharmacol Ther*. **146**, 104–119 (2015).
- Barter, P. J. *et al.* Cholesteryl ester transfer protein: a novel target for raising HDL and inhibiting atherosclerosis. *Arterioscler Thromb Vasc Biol*. **23**, 160–167 (2003).
- Tall, A. R. Plasma cholesteryl ester transfer protein. *J Lipid Res*. **34**, 1255–1274 (1993).
- Okamoto, H. *et al.* A cholesteryl ester transfer protein inhibitor attenuates atherosclerosis in rabbits. *Nature*. **406**, 203–207 (2000).
- Li, X., Catalina, F., Grundy, S. M. & Patel, S. Method to measure apolipoprotein B-48 and B-100 secretion rates in an individual mouse: evidence for a very rapid turnover of VLDL and preferential removal of B-48- relative to B-100-containing lipoproteins. *J Lipid Res*. **37**, 210–220 (1996).
- Brousseau, M. E. & Hoeg, J. M. Transgenic rabbits as models for atherosclerosis research. *J Lipid Res*. **40**, 365–375 (1999).
- Rashid, S. *et al.* Expression of human hepatic lipase in the rabbit model preferentially enhances the clearance of triglyceride-enriched versus native high-density lipoprotein apolipoprotein A-I. *Circulation*. **107**, 3066–3072 (2003).
- Wang, Z., Gerstein, M. & Snyder, M. RNA-Seq: a revolutionary tool for transcriptomics. *Nat Rev Genet*. **10**, 57–63 (2009).
- Nagalakshmi, U., Waern, K. & Snyder, M. RNA-Seq: a method for comprehensive transcriptome analysis. *Curr Protoc Mol Biol*. Chapter 4, Unit 4.11, 1–13 (2010).
- Bachorik, P. S. & Ross, J. W. National Cholesterol Education Program recommendations for measurement of low-density lipoprotein cholesterol: Executive summary. *Clin Chem*. **41**, 1414–1420 (1995).
- Nissen, S. E. *et al.* Reversal of Atherosclerosis with Aggressive Lipid Lowering (REVERSAL) Investigators. Statin therapy, LDL cholesterol, C-reactive protein, and coronary artery disease. *N Engl J Med*. **352**, 29–38 (2005).
- Austin, M. A. *et al.* Low-density lipoprotein subclass patterns and risk of myocardial infarction. *JAMA*. **260**, 1917–1921 (1988).
- Krauss, R. M. Lipoprotein subfractions and cardiovascular disease risk. *Curr Opin Lipidol*. **21**, 305–311 (2010).

18. Hoefner, D. M. *et al.* Development of a rapid, quantitative method for LDL subfractionation with use of the Quantimetrix Lipoprint LDL System. *Clin Chem.* **47**, 266–274 (2001).
19. Mertens, A. & Holvoet, P. Oxidized LDL and HDL: antagonists in atherothrombosis. *FASEB J.* **15**, 2073–2084 (2001).
20. Krauss, R. M. Dense low density lipoproteins and coronary artery disease. *Am J Cardiol.* **75**, 53B–57B (1995).
21. Gentile, M. *et al.* ApoB, small-dense ldl and carotid atherosclerosis in menopausal women. *Atherosclerosis Suppl.* **10**, S12–S12 (2009).
22. Gentile, M. *et al.* Association between small dense LDL and early atherosclerosis in a sample of menopausal women. *Clin Chim Acta.* **426**, 1–5 (2013).
23. Moore, K. J. & Tabas, I. Macrophages in the pathogenesis of atherosclerosis. *Cell.* **145**, 341–355 (2011).
24. Doran, A. C., Meller, N. & McNamara, C. A. Role of smooth muscle cells in the initiation and early progression of atherosclerosis. *Arterioscler Thromb Vasc Biol.* **28**, 812–819 (2008).
25. Tannock, L. R. *et al.* Cholesterol feeding increases C-reactive protein and serum amyloid A levels in lean insulin-sensitive subjects. *Circulation.* **111**, 3058–3062 (2005).
26. Yu, Q. *et al.* C-reactive protein levels are associated with the progression of atherosclerotic lesions in rabbits. *Histol Histopathol.* **27**, 529–535 (2012).
27. Brunt, E. M. *et al.* Nonalcoholic steatohepatitis: a proposal for grading and staging the histological lesions. *Am J Gastroenterol.* **94**, 2467–2474 (1999).
28. Kleiner, D. E. *et al.* Design and validation of a histological scoring system for nonalcoholic fatty liver disease. *Hepatology.* **41**, 1313–1321 (2005).
29. Kleemann, R. *et al.* Atherosclerosis and liver inflammation induced by increased dietary cholesterol intake: a combined transcriptomics and metabolomics analysis. *Genome Biol.* **8**, R200 (2007).
30. Wang, Z. *et al.* Hyperlipidemia-associated gene variations and expression patterns revealed by whole-genome and transcriptome sequencing of rabbit models. *Sci Rep.* **6**, 26942 (2016).
31. Karasawa, T. *et al.* Sterol regulatory element-binding protein-1 determines plasma remnant lipoproteins and accelerates atherosclerosis in low-density lipoprotein receptor-deficient mice. *Arterioscler Thromb Vasc Biol.* **31**, 1788–1795 (2011).
32. Demoulin, J. B. *et al.* Platelet-derived growth factor stimulates membrane lipid synthesis through activation of phosphatidylinositol 3-kinase and sterol regulatory element-binding proteins. *J Biol Chem.* **279**, 35392–35402 (2004).
33. Yokota, T., Nomura, K., Nagashima, M. & Kamimura, N. Fucoidan alleviates high-fat diet-induced dyslipidemia and atherosclerosis in ApoE(shl) mice deficient in apolipoprotein E expression. *J Nutr Biochem.* **32**, 46–54 (2016).
34. Wymann, M. P. & Schneider, R. Lipid signalling in disease. *Nat Rev Mol Cell Biol.* **9**, 162–176 (2008).
35. Libby, P. Inflammation and cardiovascular disease mechanisms. *Am J Clin Nutr.* **83**, 456S–460S (2006).
36. Vergnes, L., Phan, J., Strauss, M., Tafuri, S. & Reue, K. Cholesterol and cholate components of an atherogenic diet induce distinct stages of hepatic inflammatory gene expression. *J Biol Chem.* **278**, 42774–42784 (2003).
37. Colotta, F. *et al.* Interleukin-1 type II receptor: a decoy target for IL-1 that is regulated by IL-4. *Science.* **261**, 472–475 (1993).
38. Pruitt, J. H. *et al.* Increased soluble interleukin-1 type II receptor concentrations in postoperative patients and in patients with sepsis syndrome. *Blood.* **87**, 3282–3288 (1996).
39. Kolodgie, F. D. *et al.* Hypercholesterolemia in the rabbit induced by feeding graded amounts of low-level cholesterol. *Methodological considerations regarding individual variability in response to dietary cholesterol and development of lesion type.* *Arterioscler Thromb Vasc Biol.* **16**, 1454–1464 (1996).
40. Bañuls, C. *et al.* Comparability of two different polyacrylamide gel electrophoresis methods for the classification of LDL pattern type. *Clin Chim Acta.* **413**, 251–257 (2012).
41. Bai, L. *et al.* Plasma High-Mannose and Complex/Hybrid N-Glycans Are Associated with Hypercholesterolemia in Humans and Rabbits. *PLoS One* **11**, e0146982 (2016).
42. Zhang, C. *et al.* A practical method for quantifying atherosclerotic lesions in rabbits. *J Comp Pathol.* **142**, 122–128 (2010).
43. Trapnell, C. *et al.* Differential gene and transcript expression analysis of RNA-seq experiments with TopHat and Cufflinks. *Nat Protoc.* **7**, 562–578 (2012).
44. Anders, S. & Huber, W. Differential expression analysis for sequence count data. *Genome Biol.* **11**, R106 (2010).

Acknowledgements

This work was supported by grants from the National Natural Science Foundation of China (81070250, 81270348) and Public Service Platform Grant from Shaanxi Province (2014FWPT-07).

Author Contributions

E.L. and J.F. designed the study. W.W., Y.C., R.W., L.B. and Y.Z. performed the experiment. W.W., Y.C., R.W. and B.L. analyzed the data. W.W. and B.L. analyzed the transcriptome data. W.W., R.W., and S.Z. wrote the manuscript.

Additional Information

Supplementary information accompanies this paper at <https://doi.org/10.1038/s41598-018-24813-1>.

Competing Interests: The authors declare no competing interests.

Publisher's note: Springer Nature remains neutral with regard to jurisdictional claims in published maps and institutional affiliations.



Open Access This article is licensed under a Creative Commons Attribution 4.0 International License, which permits use, sharing, adaptation, distribution and reproduction in any medium or format, as long as you give appropriate credit to the original author(s) and the source, provide a link to the Creative Commons license, and indicate if changes were made. The images or other third party material in this article are included in the article's Creative Commons license, unless indicated otherwise in a credit line to the material. If material is not included in the article's Creative Commons license and your intended use is not permitted by statutory regulation or exceeds the permitted use, you will need to obtain permission directly from the copyright holder. To view a copy of this license, visit <http://creativecommons.org/licenses/by/4.0/>.

© The Author(s) 2018